Application of a Lamb Wave Technique for the Non-Destructive Inspection of Composite Structures

K. Diamanti[1], J. M. Hodgkinson[1] and C. Soutis[2]

[1]Department of Aeronautics, Imperial College London, SW7 2AZ, U.K.
k.diamanti@imperial.ac.uk, j.hodgkinson@imperial.ac.uk
[2]Aerospace Engineering, The University of Sheffield, S1 3JD, U.K.
c.soutis@sheffield.ac.uk

ABSTRACT

A cost and time effective inspection strategy for in-service health monitoring of composites is demonstrated using the fundamental anti-symmetric A_0 Lamb mode at frequencies of 15-20 kHz. In principle, this method involves analysis of the transmitted and/or reflected wave after interacting with the test-piece boundaries or discontinuities (defects). In the present work, the applicability of the technique to inspect sandwich and repaired composite structures is explored.

1. INTRODUCTION

Composite materials are prime candidates for structural applications because of their high specific strength and stiffness but are expensive to maintain. The cost of inspection is approximately one third of the total cost of manufacturing and operating composite structures [1]. In order to realize their full potential it is essential that they are maintained in a safe and economical manner.

The evaluation of structural integrity using Lamb waves has long been acknowledged as a very promising technique [2-4]. Lamb waves are two-dimensional acoustic waves that can be generated in relatively thin solid plates with free boundaries and are also known as plate waves. They can be divided into symmetric S_n and anti-symmetric A_n modes according to their displacement pattern. Lamb waves excite the whole volume of the structure along the line between the transmitter and receiver and can propagate over considerably long distances. However, their dispersive nature and the existence of many modes simultaneously can complicate the interpretation of the acquired signal.

The use of Lamb waves for the inspection of multidirectional composite laminates is well documented but less work has been done for sandwich structures. Due to the significant difference between the acoustic impedance of the core and skin and the usually high core to skin thickness ratio, the propagation of Lamb waves in sandwich structures was studied as leaky Lamb waves [5]. It was shown that the dispersion curves at low frequencies are similar to those for free plates, but the attenuation increases in the presence of the core. The S_0 mode was used at relatively high frequencies for the detection of debond between the skin and the core [5] and low velocity impact damage [6]. Operation at much lower frequencies has also shown promise for damage detection using flexural waves [7-9].

Repair techniques are regularly used in composites to restore structural integrity and prolong their life without reducing the components functionality. The use of Lamb waves for the quality assessment of adhesive joints has received considerable attention [10-12]. Koh et. al [13] used surface bonded PZTs to excite the fundamental

Lamb modes for the detection of disbond growth below a composite repair patch on an aluminium specimen. The sensors were able to detect the change in power transmission even when the damage was not located directly beneath them. A smart repair-patch with an integrated sensor network was designed by Ihn and Chang [14] to monitor crack growth in metallic structures under the composite patch. The smart layer consisted of pairs of actuators and receivers, placed on either side of the crack propagation path and was inserted into the repair-patch at different ply locations.

In this paper a cost and time effective inspection strategy using the anti-symmetric or flexural Lamb mode A_0, at low frequencies (15-20kHz) is applied to both sandwich and repaired composite structures. The wave propagation characteristics in sandwich constructions are explored and it is shown that long-range inspection can be achieved. Defects of critical size are detected and located. Repair techniques are regularly used in composites to restore structural integrity, it is therefore important for a non-destructive technique to be applicable to the structure after a repair has been undertaken.

2. EXPERIMENTAL SET-UP

Small piezoceramic patches have been selected for the generation and reception of low-frequency Lamb waves. Their low weight and volume makes them suitable for incorporation into smart structures. Operating as transmitters they transform electrical into mechanical energy. When an electrical field is applied in the direction normal to their surface, in-plane strains are mainly generated. Due to the coupling of the element to the structure, forces and moments are induced in the bonded area of the structure, generating elastic waves. As receivers they transform mechanical into electrical energy. When an elastic wave propagates through the structure the strains and stresses induced generate a voltage on the piezoceramic element. These transducers have been successfully used to excite and capture the A_0 and S_0 modes at low frequencies in other studies [9,15,16].

Rectangular piezoceramic elements, supplied by Maplin Electronics U.K. Plc. were used as transmitters or receivers. They were mounted using instant glue at one edge of the composite specimens operating in pulse-echo mode. A Pentium II personal computer and an analog-to-digital PCI-MIO-16E-1 card together with LabVIEW software by National Instruments U.K. Ltd. were used to generate the signal, excite the transmitter and subsequently acquire and process the data from the receiver. The inspection strategy described here is shown in Figure 1.

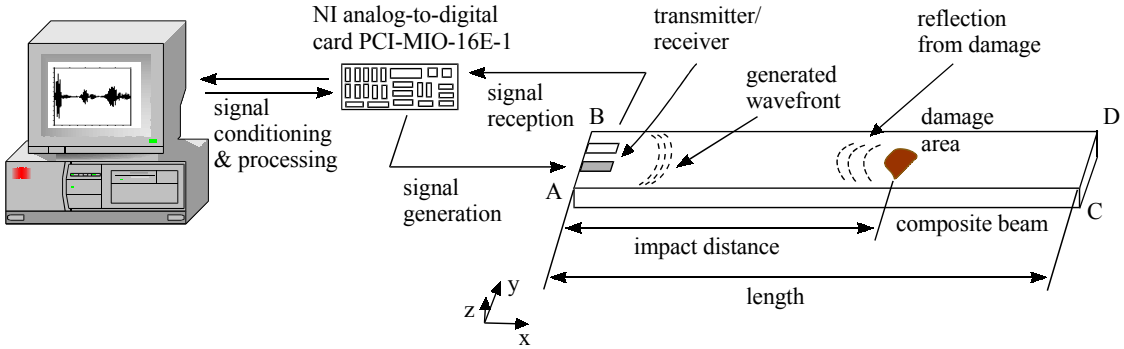

Figure 1. Schematic of the experimental set-up.

3. APPLICATIONS

3.1. Sandwich Beams

The sandwich beams consisted of 2.25 mm thick quasi-isotropic skins $[+45^o/-45^o/0^o/90^o]_{2S}$ and approximately 10 mm thick foam core. The skins were manufactured from T700UD/SE84LV carbon fibre/epoxy unidirectional pre-preg. Two types of Rohacell foam R51 and R71 (higher density) from Emkay Plastics U.K. Ltd. were used. The skins and core were post cured to form the sandwich structure using an SA80 film adhesive by SP Systems Ltd (UK). The specimens (sR51, sR71) were approximately 20 mm wide and 490 mm long.

The sandwich beams were instrumented with 6 mm wide by 20 mm long and approximately 0.1 mm thick piezoceramic elements. The transmitter was placed on one skin (side 1) and the signal was captured from two receivers bonded on both skins (sides 1 and 2) of the beam at the same edge as the transmitter. A 6.5-cycles sinusoidal pulse enclosed in a Hanning window with amplitude +/- 10 V was used to drive the transmitter. The signal was simultaneously captured from the two receivers at 1.25 MS/s sampling frequency.

A beam specimen was cut from the quasi-isotropic laminate for comparison of the wave propagation in the skin to the sandwich specimens. Figure 2 shows the signals acquired from the skin alone and from the sandwich beams (side 1) at different frequencies. It can be observed that no significant changes in the shape or the arrival time of the pulse are introduced by the presence of the foam. However, significant attenuation is present due to energy being dissipated into the core. This allows us to assume that there is leaky Lamb wave propagation [5,6]. Although attenuation is greater, the reflection from the far edge of the beam can still be detected, as can be seen in the time traces, after it has travelled twice the length of the beam, i.e. approximately 1 m. The A_0 mode at low frequencies could therefore be used for the long-range inspection of sandwich structures.

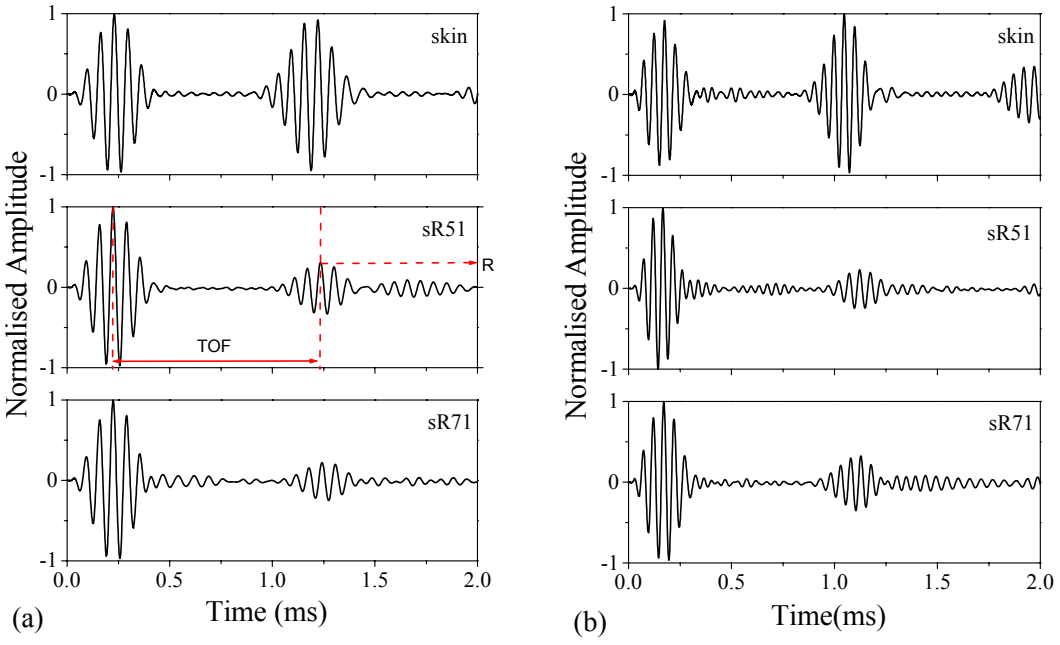

Figure 2 Signals received on the skin alone and the sandwich beams at 15 kHz (a) and 20 kHz (b).

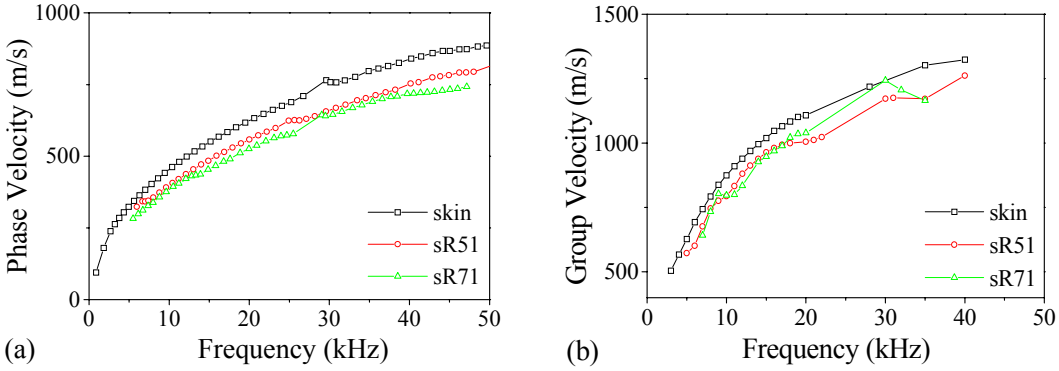

Figure 3 Experimental dispersion curves for the skin alone and the sandwich beams.

The resonant spectrum method [15] was used here to measure the phase velocity of the A_0 Lamb mode for the sandwich specimens. The group velocity was also calculated at various frequencies. The measurements were taken from the specimens having the transducer and receiver on the same side. The dispersion curves for the skin alone were also measured. The results are depicted in Figure 3. It must be noted that the velocities are plotted versus frequency and not the frequency-thickness product. It can be observed that the dispersion curves obtained for the sandwich beams were very close to those calculated for the skin, in accordance with other studies [5-8]. The difference can be attributed to the adhesive because the skin with the adhesive has lower stiffness than the skin alone. The thicker the adhesive layer the bigger the difference [5].

In an earlier paper by the authors artificial debonds of the skin to the core, induced with a sharp knife, were detected using this experimental set-up [17]. Impact tests were undertaken here to introduce more realistic damage using a 1.54 kg, 12.5 mm in diameter, hemispherical impactor. The impact point was 200 mm from the edge of the beam on side 1. A 75 mm length of the specimen was clamped having the impact point in the centre. The impact tests were repeated with higher impact energy levels until a significant amount of damage had developed. The impact area, in generally, consisted of debonding of the skin from the core, crushed core and delaminations in the skin.

Radiography was used as an alternative inspection method. No damage was evident on the X-ray images after 5 J impact in the sR51 specimen. A debond between the skin 1 and the core appeared after 10 J impact across the whole width. This ranged from 170 mm to 240 mm from the transducers location (Figure 1). For the beam with the denser foam sR71 damage first appeared at a higher impact energy level of 15 J. A debond immediately below the impact point was generated. Cracks developed at the edges of that debond in the core that propagated through the core and led to debonds on the opposite skin. Delaminated layers could also be seen at the surface of the top skin. The damage area ranged from 160 mm to 230 mm across the length of the specimen.

The response of the specimens from a 15 kHz excitation signal was captured by the two receivers. The transmitter and receiver 1 (top surface) were in line with the impact point. The second receiver 2 was on the opposite skin (bottom surface). The reflection coefficient (R) of the transmitted signal and the time of flight (TOF) from the excitation are depicted in Figure 2. These parameters were monitored for the

different stages of damage in Table 1 and Table 2. No consistent trend has been found for the amplitude of the transmitted wave. However it can be observed that the TOF increases as damage accumulates. This gives a clear indication of the extent of damage even for damage that was not detected by radiography. It is also clear that detection is achieved by both receivers, due to the way the flexural wave propagates along the sandwich structures. It travels from one skin to the other through the core, thus carrying information for the whole structure. The location of damage was predicted to be close to the true value for all the cases as can be seen in the following tables.

Table 1 Effect of impact damage in the response of the sR51 sandwich specimen. Damage location was 170 mm to 240 mm along the length.

Impact Energy (J)	Reflection Coefficient	TOF (ms)	Damage Location (mm)	Reflection Coefficient	TOF (ms)	Damage Location (mm)
		Receiver 1			Receiver 2	
0	0.243	0.938	-	0.278	0.997	-
5	0.305	0.943	-	0.287	1.002	-
10	0.137	0.996	226.7	0.455	1.026	213.0

Table 2 Effect of impact damage in the response of the sR71 sandwich specimen. Damage location was 160 mm to 230 mm along the length.

Impact Energy (J)	Reflection Coefficient	TOF (ms)	Damage Location (mm)	Reflection Coefficient	TOF (ms)	Damage Location (mm)
		Receiver 1			Receiver 2	
0	0.279	1.020	-	0.270	1.028	-
5	0.283	1.026	-	0.252	1.034	-
10	0.294	1.034	-	0.268	1.042	-
15	0.239	1.053	207.0	0.297	1.056	217.5

3.2. Repaired Composite Beams

In the current work we are concerned only with the use of external patches as a repair technique. This type of repair is widely employed since it is relatively easy to apply. It is mainly used in field repairs where rapid solutions are required and skilled personnel and adequate facilities are unavailable. The damage area is usually removed by drilling a hole and a composite plate is either bolted or adhered to the surface of the component.

The single (2.5 mm thick patch) and double lap (1.25 mm thick patches) repair specimens used here are shown in Figure 4. Both the parent specimens and patch repairs were manufactured from T700UD/SE84LV UD prepreg tapes supplied by SP Systems to form quasi-isotropic laminates. A 9 mm hole was drilled to represent the removed damaged area, using a diamond coated tip drill piece. The required overlap length was calculated through analytical expressions [18]. No tapering was used. The specimens were 475 mm long and 30 mm wide. An SA80 SP Systems adhesive was used to bond the patches on the specimens. The specimens were instrumented with a pair of 5 by 15 mm piezoceramic elements. A sampling frequency of 1.25 MS/s was used throughout the tests.

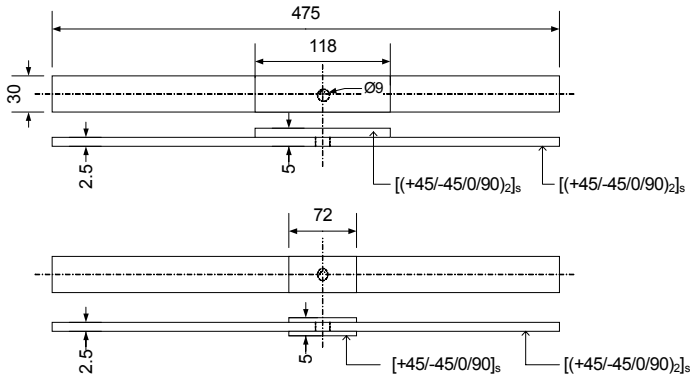

Figure 4 Geometry of repair specimens; dimensions in mm.

Figure 5 shows the signals received from the double lap repair specimen being excited by a 5.5 cycle sinusoidal pulse in a Hanning window at 15 kHz and 20 kHz. At the frequency of 15 kHz it was observed that the reflections from the two ends of the patch could not be separated and are seen as the signal 3 in Figure 5 (a). However, at the higher frequency, Figure 5 (b), the smaller wavelength permitted a visible time separation between the two pulses seen as signals 3 and 4. Therefore the higher frequency was selected for the inspection of the repair specimens. Similar results were observed in the single lap repair specimen.

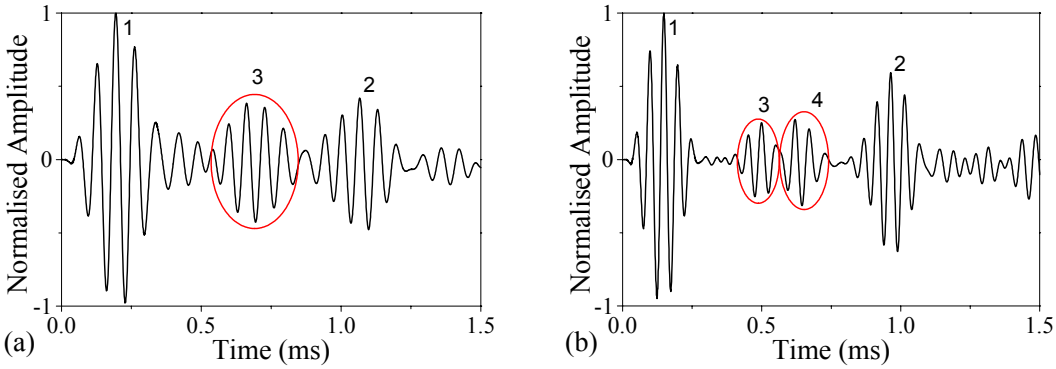

Figure 5 Response of the double lap repair specimen at (a) 15 kHz and (b) 20 kHz.

Figure 6 shows a schematic of the single lap repair specimen and the cross correlation coefficient of the monitored response, which is calculated as the product of the excitation pulse with the response of the structure at every time step. In general, when there is a crack below the patch, the propagation path of the wave in the parent specimen increases while the path in the repaired area of the specimen decreases. The wave propagates in the patched specimen at a higher velocity as the thickness at that point is double that of the parent specimen. Therefore in the cracked specimen the length of the parent specimen with the lower velocity increases and that causes the signal travelling through the whole propagation distance to be delayed. As the crack grows from point B to B' (crack length is BB') the peak of signal B will also be delayed. Finally the time that signal C appears depends on the length of both cracks and the relative difference between the velocities of the patched and parent specimen. If there is no debond at the beginning of the patch and the crack has only grown at the end (crack length is CC ') the signal C will appear sooner.

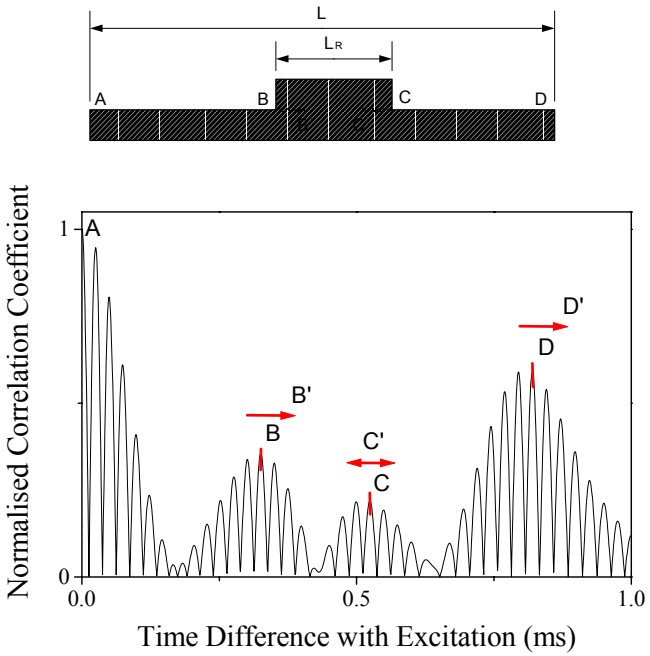

Figure 6 Schematic of the single lap repair specimen and the acquired Lamb wave response.

A Finite Element model was built in Abaqus 6.3 [19] to check the TOF behaviour described above. In the analysis 4 noded general shell elements were used for the parent specimen. The patch was also modelled with shell elements on top of the parent specimen using multipoint constraints at the common nodes. A single lap repair specimen was built having the same dimensions as the test specimen. Nodes were disconnected gradually to obtain the response of the cracked structure. Cracks were introduced at the first edge of the patch and the TOF changes between the signals A and B are plotted against the crack length in Figure 7 (a). Deviation from the linear behaviour is expected due to the difficulty of identifying the peak of the signals at low frequency. However, a clear indication of the debond growth below the patch is shown from the delay in the signal. In Figure 7 (b) the crack was gradually increased from side 2 and the TOF between signals C and D is plotted against the crack length.

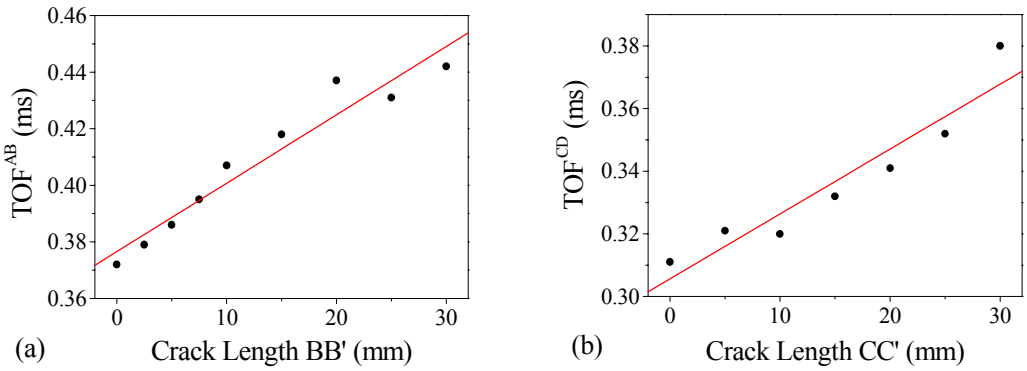

Figure 7 TOF increase with increasing crack length (a) in the beginning (BB') and (b) end of the patch (CC') from FE analysis.

In order to introduce a crack underneath the patch, 4-point bending experiments were undertaken. The testing fixture consisted of two parts, each having two movable cylindrical surfaced noses. The specimens were fixed at two points, 150 mm apart for the specimens with the shorter patch and 200 mm apart for the longer one, the patch was located centrally at the support span. The two loading points were spaced 25 mm away from their adjacent support point for all the specimens. The support span was 100 mm and 150 mm for the shorter and longer patch respectively. The load was applied at a rate of 1 mm/min until a crack appeared at the skin-patch interface. In order to assist the reading of the crack length the sides of the specimens were painted white and markings were printed at 1 mm intervals.

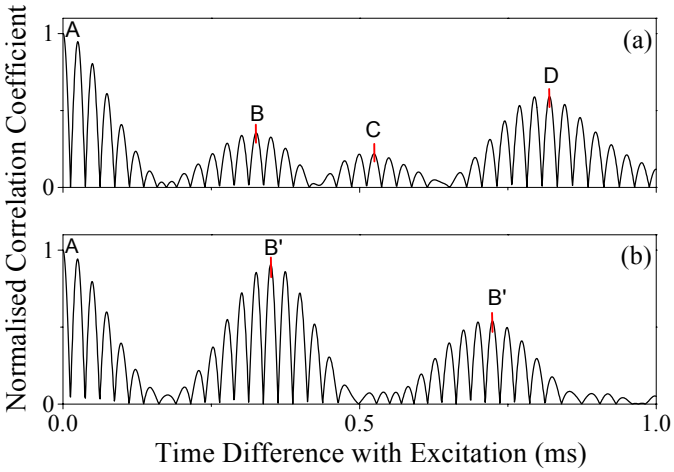

Figure 8 Response of the pristine (a) and damaged (b) single lap repair specimen.

The cross correlation between the excitation pulse and response of the structure was computed to identify the time difference between the separate wave packets. Figure 8 (a) shows the response of the undamaged single lap repair specimen. The group velocities were experimentally measured for the parent specimen of the same lay-up and material at different frequencies and are reported in Table 3. Using these values and the TOF measurements, the length of the various areas in the repaired specimen can be calculated. The results are given in Table 4. Good correlation is achieved for the AB and CD distance but agreement was poor for the BC distance. This is because the velocity used for the wave propagation in that region was taken from the parent material without the adhesive. The presence of the adhesive will decrease the stiffness and therefore the flexural wave velocity in that region.

After the test the cracks BB' and CC' were measured with a magnifying camera, 10 mm and 18 mm, respectively. The response of the damaged specimen is depicted in Figure 8 (b). It can be observed that a very strong signal was reflected from the crack BB' which travelled back and forth within the AB distance causing repeated reflections. The estimated crack length was 12 mm instead of 10 mm as given in Table 4. Little energy was transmitted to the rest of the specimen and the signals from points C and D were not recorded, therefore no information is given for the other end of the patch.

The differences in the TOF of the individual signals for the double lap repair specimen and the predicted cracks are given in Table 5. The time difference between

the signals from the edge of the beam A or D and the patch B or C correspond to the lengths AB and CD respectively, Figure 6. When a crack is present the TOF increases. That is attributed to the wave propagation along the cracked part of the specimen, BB' or CC'. In this specimen cracks appeared only in the side of the patched specimen that was in tension. Therefore the velocity for the 3.75 mm thick part of the specimen at 75 kHz mm frequency thickness product was used to calculate the crack length. Good estimation of the crack growth is achieved which is consistent for both specimens.

Table 3 Experimental values of the group velocity from the 2.5 mm thick quasi-isotropic beam.

fh (kHz mm)	Cg (m/s)
25	898
50	1159
75	1288
100	1355

Table 4 Predicted debond in the single lap repair specimen.

Distance	TOF (ms)	Estimated value (mm)	Actual value (mm)
AB	0.326	189	191
BC	0.198	134	118
CD	0.296	172	166
AB'	0.350	203	201

Table 5 Predicted debond in the double lap repair specimen.

Distance	TOF (ms)	Distance	TOF (ms)	Difference (μs)	Predicted crack length (mm)	Actual crack length (mm)
AB	0.347	AB'	0.353	6	3.9	5
CD	0.313	C'D	0.318	5	3.2	3

4. CONCLUDING REMARKS

The A_0 Lamb wave propagation in sandwich structures has been studied at low-frequencies (10-50 kHz). At least 10 % of the amplitude of the excited signal was monitored after 1 m of propagation distance, which shows that the technique is applicable for the inspection of relatively long sandwich structures. Changes in the response of the propagated pulses have been used to detect and locate impact damage. The technique could be used to inspect damage that is located in any position though the thickness even if only one side is accessible for testing.

It is shown that the low-frequency Lamb waves could be successfully used to interrogate composite structures after a repair has been undertaken. The technique is very sensitive to small changes of the structural integrity of the repaired structures. Hairline cracks below the patch as small as 3 mm in length were successfully detected. Tapering of the patch should be investigated as it will affect the wave reflection from the patch edges. However, when cracks have initiated it is thought that the behaviour is going to be similar to that described here.

References

1. **Bar-Cohen, Y.**, ″Emerging NDE Technologies and Challenges at the Beginning of the 3 rd Millennium -- Part II″, NDT.net, **5**/2 (2000), 1-10.
2. **Lamb, H.**, "On Waves in an Elastic Plate″, Proceedings of the Royal Society of London, (1917), 114-128.
3. **Worlton, D.C.**, ″Ultrasonic Testing with Lamb Waves″, NonDestructive Testing, **15**/4 (1957), 218-222.
4. **Cawley, P.**, ″The Rapid Non-Destructive Inspection of Large Composite Structures″, Composites, **25**/5 (1994), 351-357.
5. **Guo, N.** and **Lim, M.K.**, ″Lamb Waves Propagation in Aluminium Honeycomb Structures″, Review of Progress in Quantitative Nondestructive Evaluation, Thompson, D.O. and Chimenti, D.E., New York, Plenum Press, **15** (1996), 323-330.
6. **Bourasseau, N.**, **Moulin, E.**, **Delebarre, C.** and **Bonniau, P.**, ″Radome Health Monitoring with Lamb Waves: Experimental Approach″, NDT&E International, **33**/6 (2000), 393-400.
7. **Osmont, D.**, **Devillers, D.** and **Taillade, F.**, ″Health Monitoring of Sandwich Plates Based on the Analysis of the Interaction of Lamb Waves with Damages″, Proceedings of SPIE Smart Structures and Material 2001: Smart Structures and Integrated Systems, Davis, L.P., SPIE, **4327** (2001), 290-301.
8. **Osmont, D.**, **Barnoncel, D.**, **Devillers, D.** and **Dupont, M.**, ″Health Monitoring of Sandwich Plates Based on the Analysis of the Interaction of Lamb Waves with Damages″, Proceedings of the First European Workshop of Structural Health Monitoring, Balageas, D., USA, DEStech Publications, (2002), 336-343.
9. **Kessler, S.S.**, **Spearing, S.M.** and **Soutis, C.**, ″Damage Detection in Composite Materials using Lamb Wave Methods″, Smart Materials and Structures, **11**/2 (2002), 269-278.
10. **Mal, A.K.**, **Xu, P.C.** and **Bar-Cohen, Y.**, ″Analysis of Leaky Lamb Waves in Bonded Plates″, Int. J. Engng Sci., **27**/7 (1989), 779-791.
11. **Rokhlin, S.I.**, ″Lamb Wave Interaction with Lap-Shear Adhesive Joints: Theory and Experiment″, J. Acoust. Soc. Am., **89**/6 (1991), 2758-2765.
12. **Lowe, M.J.S.** and **Cawley, P.**, ″The Applicability of Plate Wave Techniques for the Inspection of Adhesive and Diffusion Bonded Joints″, Journal of Nondestructive Evaluation, **13**/4 (1994), 185-200.
13. **Koh, Y.L.**, **Chiu, W.K.** and **Rajic, N.**, ″Integrity Assessment of Composite Repair Patch Using Propagating Lamb Waves″, Composite Structures, **58** (2002), 363-371.
14. **Ihn, J.B.** and **Chang, F.K.**, ″A Smart Patch for Monitoring Crack Growth in Metallic Structures Underneath Bonded Composite Repair Patches″, Proc. of Am. Soc. Comp., Sun, C.T. and Kim, H., **17** (2002),
15. **Díaz Valdés, S.H.** and **Soutis, C.**, ″Real-Time Nondestructive Evaluation of Fibre Composite Laminates Using Low-Frequency Lamb Waves″, J. Acoust. Soc. Am., **111**/5 (2002), 2026-2033.
16. **Giurgiutiu, V.**, **Zagrai, A.** and **Bao, J.J.**, ″Piezoelectric Wafer Embedded Active Sensors for Aging Aircraft Structural Health Monitoring″, Structural Health Monitoring, **1**/1 (2002), 41-61.
17. **Diamanti, K.**, **Soutis, C.** and **Hodgkinson, J.M.**, ″Lamb Waves for the Non-Destructive Inspection of Monolithic and Sandwich Composite Beams″, Presented in the DFC7, April 2003, Sheffield, U.K., to be published in Composites: Part A.
18. ″Joining Fibre - Reinforced Plastics, edited by F. L. Mathews″, England, Elsevier Applied Science, (1987).
19. ″ABAQUS®, Theory Manual, Version 5.8″, U.S.A.